Individual Block Length Distributions of Block Copolymers of Polystyrene-*block*-Poly(α-methylstyrene) by MALDI/TOF Mass Spectrometry

Grazyna Wilczek-Vera,[†] Paul O. Danis,[‡] and Adi Eisenberg*[,†]

Department of Chemistry, McGill University, 801 Sherbrooke Street West, Montréal, Québec, Canada H3A 2K6, and Rohm and Haas Company, Research Laboratories, Spring House, Pennsylvania 19477

Received October 31, 1995[⊗]

ABSTRACT: The block length distributions of two block copolymers of α-methylstyrene and styrene, of different molecular weights and relative block lengths, were analyzed by matrix-assisted laser desorption/ionization time-of-flight (MALDI/TOF) mass spectrometry. A method for the treatment of mass spectroscopic data for block copolymers is proposed. The random coupling hypothesis has been verified experimentally and found to hold for this type of triblock copolymers. The experimental distributions have been compared with the Poisson and Schulz−Zimm models modified to accommodate the change of variables. The agreement between the experimental and calculated distributions is very good for the Schulz−Zimm model and fair for the Poisson model. Mass spectrometry proved to be a useful technique providing unique information on the experimental distributions of **both** constituent parts in a block copolymer. It was confirmed that block copolymers with narrow molecular weight distributions may have broad, complex, and even bimodal composition distributions. The polydispersity factors observed for the individual parts were higher than those for the whole copolymer.

Introduction

In the recent past, there has been a considerable upswing and interest in properties of block copolymers. Micellization, brush formation, and drug delivery are just three examples of the areas in which block copolymers have been receiving extensive attention. For the study of many of these properties, detailed information about the block lengths and compositions of each of the segments is needed. However, while it has been possible to determine the total molecular weight and the molecular weight distribution of the block copolymer, as well as the molecular weight and molecular weight distribution of the first segment to be prepared,[1,2] it has not been possible, with the exception of few cases,[3−5] to determine independently the molecular weight and molecular weight distribution of the second segment. This information can be of considerable importance, since, to pick one example, it has recently been shown that the size of the core of block copolymer micelles is very much a function of the molecular weight distribution of the core forming block.[6] In the above case, the core forming block was composed of vinylpyridinium methyl iodide, while the corona consisted of styrene. In that case, the block length distribution was broadened artificially to obtain very large values of the heterogenity index. However, in general, it has been impossible to obtain detailed data on the second block (e.g., vinylpyridine) independent of the first (e.g., styrene). A number of theoretical treatments exist which make possible the calculation of the molecular weight distribution of the second block from the molecular weight distribution of the first block and of the total block copolymers. These methods are very useful for some compositions, but, if the first block is sizable and the second block is relatively small, the error associated with the applications of this method can be appreciable.

The advent of mass spectrometry techniques, which give molecular masses up to the range of ca. 10 000, has opened the possibility of the investigation of detailed block copolymer compositions in that range of molecular weights.[7,8] Specifically, matrix-assisted laser desorption/ionization time-of-flight mass spectrometry (MALDI/TOF) has yielded very satisfactory information for polymers in that molecular weight range.[9] However, a detailed analysis of the data for block copolymers is required in order to obtain meaningful numbers for the molecular weight distribution and the compositional distribution of the specific samples. These, as will be shown below, are by no means straightforward.

The purpose of this paper, therefore, is to demonstrate the utility of the mass spectroscopic technique for the study of block copolymers. Specifically, the method is applied to study the molecular weights and molecular weight distributions of **both** components of a block copolymer. Methods are suggested to obtain required information from the treatment of mass spectroscopic data. Existing equations from published distribution models are modified to make them easily applicable to block copolymers. Finally, a detailed comparison is made between the experimental composition distributions obtained for two samples of a specific block copolymer system, styrene−α-methylstyrene, with a theoretically derived distribution function, i.e., the Schulz-Zimm (Γ) model.

Experimental Section

The Synthesis. The block copolymer was prepared by sequential anionic polymerization, with secondary butyllithium used as the initiator. A small amount of α-methylstyrene (component A) was added to the initiator mixture upon which the color turned red, typical of the α-methylstyrene anion. Styrene (component B) was then added to the reaction mixture and the polymerization was allowed to proceed until the styrene was exhausted. During the styrene polymerization, the color of the solution was yellow, characteristic of the styrene anion. Once the styrene was polymerized, the color turned back to the red, characteristic of the α-methylstyrene anion. It should be recalled that α-methylstyrene, at room temperature and under conditions normally used for anionic polymerization, i.e., in dilute solutions, is above its ceiling temperature, so that high molecular weights of α-methylsty-

[†] McGill University.
[‡] Rohm and Haas Company.
[⊗] Abstract published in *Advance ACS Abstracts,* May 1, 1996.

S0024-9297(95)01639-1 CCC: $12.00

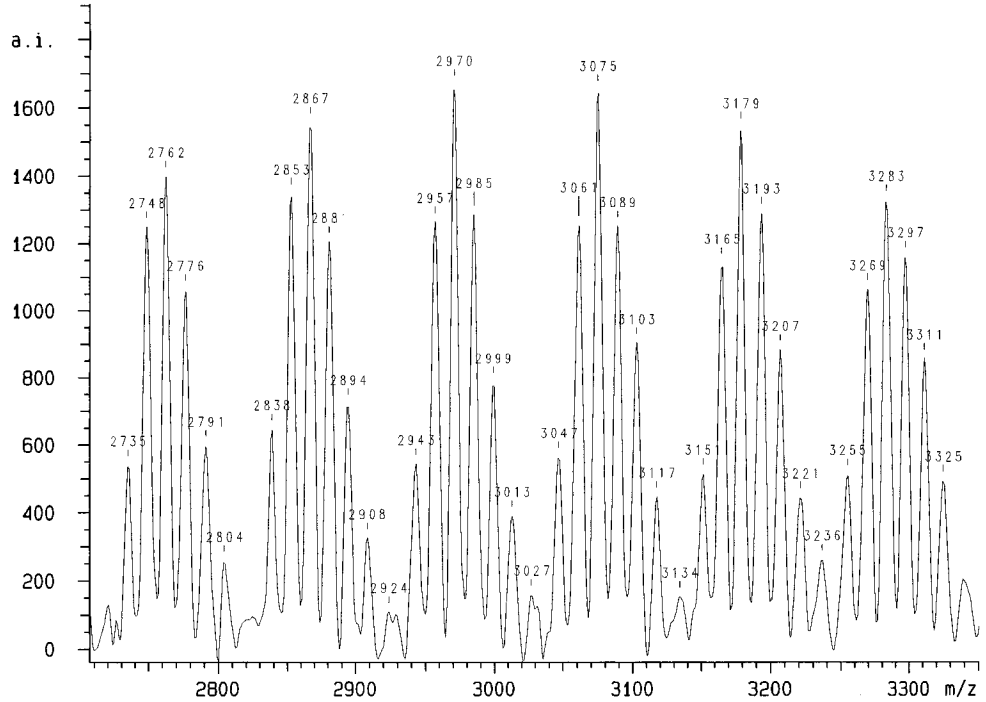

Figure 1. Enlarged detail of the MALDI/TOF mass spectrum of sample I.

rene are not obtainable. Hence, in the present method of synthesis, the butyl segment is followed by a short α-methylstyrene segment, which in turn is followed by the styrene segment and, finally, another short segment of α-methylstyrene before the chain is terminated. Methanol was used to terminate the chains. Thus, for the purpose of the subsequent discussion, it is important to remember that an α-methylstyrene segment is present at the beginning of the chain after the butyl group as well as at the end of the chain, i.e., that a triblock copolymer, ABA, is formed.

Mass Spectrometry. MALDI/TOF measurements were performed on a Bruker (Billerica, MA) REFLEX mass spectrometer, operating in the reflector mode. Details of the instrument are given elsewhere.[9] The matrix was prepared by mixing 40 mg of *trans*-3-indoleacrylic acid (Aldrich, Milwaukee, WI) and 40 mg of silver acetylacetonate (Aldrich, Milwaukee, WI) in 5 mL of methanol and sonicating for 30 min. The solution was filtered (0.2 μm) and the filtrate was dried. The dried filtrate was dissolved in tetrahydrofuran (THF) at a concentration of 3 mg/100 μL. The polymer was dissolved in THF at a concentration of 4 mg/mL and 4 μL of polymer solution was mixed with 20 μL of matrix solution. This polymer−matrix solution was shaken briefly and 2 μL were applied to the probe. Ions were formed by laser desorption at 337 nm (N_2 laser, 3-ns pulse width, 10^6 to 10^7 W/cm^2, 100-μm diameter spot), accelerated to 30 kV and detected as positive ions. The spectra are the sum of 200−300 laser shots acquired at 5-Hz repetition rate. Spectra were baseline corrected and smoothed with a three-point Golay-Sawitski smoothing algorithm. An external calibration using bovine insulin and angiotension II (Sigma, St. Louis, MO) was used.

Size Exclusion Chromatography. The SEC measurement was performed at 35 °C on a Varian 5010 liquid chromatograph equipped with a refractive index detector. THF was used as eluent at a flow rate of 1 mL/min. The column was an Ultrastyragel 10*410**5. The system was calibrated with monodisperse polystyrene. The concentration of injected polymer solution was 0.5 mg/mL. The solution was filtered through membrane filters before injection. The number and weight average molecular weight of the polystyrene block and the copolymer were calculated by a Varian DS-604 with SEC application software. The possibility of adsorption of the polymer by the column will be discussed later.

Results and Discussion

Experimental Data. Two samples of a block polymer of polystyrene−poly-(α-methylstyrene), differing in their average molecular weights and composition, were analyzed. Figure 1 presents, as an example, an enlarged portion of the sample I spectrum near its maximum intensity. The complete spectrum of this sample extends on the m/z axis from 2250 to 3845, with the maximum intensity at 2970. The spectrum of sample II covers the range of m/z values between 2700 and 6200, with the maximum intensity at 4168.

The intensity values of peaks were obtained by integrating the area under the peaks. The digital values were used for further calculations. Occasionally, the software used for the area peak determination experienced some difficulties with the detection of peaks due to resolution problems, in that the intensity values reported were too high. These obvious errors were corrected by comparing the peak areas with the original graphical spectrum.

Identification of Peaks. As was discussed before, each molecule of a block copolymer contained one butyl group (molecular weight $M^0_{\text{butyl}} = 57.115$), one hydrogen ($M_{\text{H}} = 1.008$), a few segments of α-methylstyrene (molecular weight $M^0_{\text{A}} = 118.18$), and many segments of styrene (molecular weight $M^0_{\text{B}} = 104.15$). Additionally, during ionization, one silver cation ($M_{\text{Ag}} = 107.868$) becomes attached to form the molecular ion of the oligomer. Therefore, it was possible to find the number of segments n_{A} and n_{B} in a molecule by comparing the experimental value of m/z with the calculated molecular weight:

$$(m/z)_{\text{calc}} = n_{\text{A}}M^0_{\text{A}} + n_{\text{B}}M^0_{\text{B}} + (M^0_{\text{butyl}} + M_{\text{Ag}} + M_{\text{H}}) \quad (1)$$

For this purpose, a sizable matrix of $(m/z)_{\text{calc}}$ values were obtained, covering the whole reasonable range of variability of the numbers of segments n_{A} and n_{B}. It was assumed that n_{A} could change from 1 to 35, while n_{B} from 4 to 56. The calculated values of m/z were

Table 1. Possible Assignments of the Chemical Composition for the Strongest Peak in Sample I (m/z = 2970.5)

$(m/z)_{calc}$	n_A	n_B	$\Delta = (m/z)_{calc} - (m/z)_{exp}$
2965.2	14	11	−4.3
2971.1	7	19	1.6
2979.2	15	10	9.7

compared with the experimental values of m/z. One should point out that eq 1 contains two variables, the numbers of segments n_A and n_B. Therefore, additional information on the chemical composition of the sample is required to choose a physically meaningful solution.

Let us first discuss sample I. The strongest peak in this sample was observed at 2970.5 (see Figure 1). The three closest values of m/z, calculated from eq 1, are listed in Table 1. The calculated m/z value of 2971.1, with the corresponding values $n_A = 7$ and $n_B = 19$ was chosen, because it produces the smallest deviation from the experimental value of m/z. Additionally, the chemical composition obtained agrees with our knowledge on the composition of this block copolymer (the molar ratio of α-methylstyrene to styrene is less than one). This second piece of information is always necessary due to the character of the problem (two variables, one equation).

Once the chemical composition of the strongest peak was assigned, the characterization of other peaks was simple. Two properties of the acquired MS spectrum were used (see Figure 1):

1. The differences in the experimental values of m/z between the strongest peaks in the neighboring groups of peaks is about 104 ± 2 (e.g., 2762, 2867, 2970, 3075, 3179, 3283, etc.). This corresponds roughly to the molecular weight of styrene ($M_B^0 = 104.15$). It means that these peaks have the same value of n_A, while the value of n_B increases by 1 when passing from the lower values of m/z to the higher values of m/z.

2. The difference between the neighboring peaks within a group of peaks (e.g., 2943, 2957, 2970, 2985, 2999, 3013, 3027) is about 14. This corresponds to the difference in the molecular weight of α-methylstyrene ($M_A^0 = 118.18$) and styrene (molecular weight $M_B^0 = 104.15$). It means that in a group of peaks with increasing mass, the values of n_A are increasing and values of n_B are decreasing.

These rules were applied to resolve the structure of the mass spectrum of the first sample. As an example, the assignment of peaks for the two central groups of peaks, i.e., around the peaks at $m/z = 2970$ and 3075, is presented in Table 2.

The assignment of the chemical composition in the second sample was more difficult. As the average molecular weight of a polymer increases, the number of possible combinations of n_A and n_B, that can satisfy eq 1, increases. Table 3 presents different calculated values of m/z that reproduce well the experimental value of $m/z = 4168.1$ recorded for the strongest peak in sample II.

It is clear from the results presented in Table 3 that it is not possible to decide from this table alone which assignment of n_A and n_B values should be chosen. At least two combinations of (n_A,n_B) seem possible: (3,35) and (18,18). Therefore, as an independent indication of the block copolymer composition, the ^{1}H-NMR spectra of both copolymers were obtained. These data provided a second constraint, relating the two variables, n_A and n_B. Table 4 presents the results of the NMR analysis.

Table 2. Assignments of the Chemical Composition for Two Central Groups of Peaks in Sample I

$(m/z)_{exp}$	n_A	n_B	$\Delta = (m/z)_{calc} - (m/z)_{exp}$	integral intensity
First Group of Peaks				
2942.9	5	21	1.1	3865
2956.5	6	20	1.6	9442
2970.5	7	19	1.6	11760
2984.7	8	18	1.4	9077
2998.8	9	17	1.3	5285
3012.6	10	16	1.6	2552
3027.0	11	15	1.2	1239
Second Group of Peaks				
3046.7	5	22	1.5	4070
3060.8	6	21	1.4	9124
3074.5	7	20	1.7	11744
3088.7	8	19	1.6	9017
3102.5	9	18	1.8	6481
3117.2	10	17	1.1	2848
3134.0	11	16	−1.7	1589

Table 3. Possible Assignments of the Chemical Composition for the Strongest Peak in Sample II (m/z = 4168.1)

$(m/z)_{calc}$	n_A	n_B	$\Delta = (m/z)_{calc} - (m/z)_{exp}$
4161.0	25	10	−6.2
4164.8	3	35	−2.3
4166.9	18	18	−0.2
4172.9	11	26	5.8

Table 4. Molecular Composition of Analyzed Samples as Determined by the ^{1}H-NMR Spectroscopy

	mol % of[a]	
	α-methylstyrene	styrene
sample I	31%	69%
sample II	17%	83%

[a] The contribution of the butyl group was neglected during the calculations. Its contents in sample I was estimated to be around 3.5% (mol/mol) and in sample II 2.4% (mol/mol).

Table 5. Summary of the Peak Assignment for Samples I and II

	sample I	sample II
no. of peaks	136	232
av Δ[a]	1.6	−1.5
standard deviation of Δ	1.1	2.8
mol % of α-methylstyrene	29%	13%

[a] $\Delta = (m/z)_{calc} - (m/z)_{exp}$.

Since the results of the NMR spectroscopy showed that there was much more styrene (component B) in the sample than α-methylstyrene (component A), the second solution ($n_A = 3$, $n_B = 35$) was chosen. Then, the further assignment was performed following the same rules as for sample I.

After the values of n_A and n_B were assigned to all the peaks in samples I and II, all the experimental intensities (peak areas) were normalized by dividing each peak intensity by the sum of all the intensities recorded for a particular sample. As the normalized peak intensity corresponds to the probability of occurrence of a particular combination of n_A and n_B, these relative intensity values could be used to calculate the molar content of components A and B in a sample and, by comparison with the data obtained from NMR, confirm the correctness of the assessment. Table 5 presents these results for both samples. It also summarizes the deviations between the experimental and calculated values of m/z.

Taking into account that the accuracy of the molecular composition for the first sample, as determined by

Table 6. Parameters Characterizing the Size of the Matrix of Relative Intensities (Probabilities) for Samples I and II

	sample I		sample II	
	block A	block B	block A	block B
n_j^{min}	4	8	2	8
n_j^{max}	11	36	10	51
N_j	8	25	9	44

the ^{1}H-NMR spectroscopy, is less than 3.5% (mol/mol) and, for the second sample, is less than 2.4% (mol/mol), one can accept as satisfactory the agreement between the molar contents of α-methylstyrene obtained by the NMR and the MS spectrometry. This validates the performed assessment of the MS peaks.

It is also interesting to compare the calculated mole percent of α-methylstyrene for two other combinations of n_A and n_B reported in Table 3. For the sequence (n_A = 18, n_B = 18), this mole fraction is 50%. For the combination (n_A = 11, n_B = 26), the result is 47%. Both values are quite different from the NMR data.

Experimental Distribution of Units. After the assignment of specific values of n_A and n_B to all the experimental peaks was done, the resulting data were organized in the following matrix:

peak no.	m/z	n_A	n_B	relative intensity (probability)
1	(m/z)	n_1^A	n_1^B	$\Gamma_{exp}(n_1^A,n_1^B)$
...	...	...	...	...
k	$(m/z)_k$	n_k^A	n_k^B	$\Gamma_{exp}(n_k^A,n_k^B)$

This matrix was rearranged by grouping all the probabilities corresponding to the same n_A in one column and probabilities with the same n_B in one row. The resulting matrix of relative intensities (probabilities) $\Gamma_{exp}(n_{i_A}^A,n_{i_B}^B)$, had the following structure:

	column no. →	1		i_A		N_A
row no. ↓		$n_A = n_A^{min}$	...	$n_A = n_{i_A}^A$	...	$n_A = n_A^{max}$
1	$n_B = n_B^{min}$	$\Gamma_{exp}(n_1^A,n_1^B)$	...	$\Gamma_{exp}(n_{i_A}^A,n_1^B)$	...	$\Gamma_{exp}(n_{N_A}^A,n_1^B)$
	...	...	...	...	...	
i_B	$n_B = n_{i_B}^B$	$\Gamma_{exp}(n_1^A,n_{i_B}^B)$	...	$\Gamma_{exp}(n_{i_A}^A,n_{i_B}^B)$		$\Gamma_{exp}(n_{N_A}^A,n_{i_B}^B)$
	...	...	...	...	...	
N_B	$n_B = n_B^{max}$	$\Gamma_{exp}(n_1^A,n_{N_B}^B)$	...	$\Gamma_{exp}(n_{i_A}^A,n_{n_B}^B)$		$\Gamma_{exp}(n_{N_A}^A,n_{N_B}^B)$

As n_A can vary from n_A^{min} to n_A^{max}, and the range of variability for n_B is from n_B^{min} to n_B^{max}, the dimension of the matrix is ($N_A \times N_B$), where $N_j = n_j^{max} - n_j^{min} + 1$ (j = A, B). All parameters characterizing the size of the matrix of relative intensities (probabilities) for the samples I and II are reported in Table 6.

Sample I contained from 4 to 11 units of α-methyl styrene and from 8 to 36 units of styrene. As the matrix contains 8 × 25 = 200 elements, it is clear that 136 recorded peaks left some empty spaces. The same is true for the second sample. This sample contains from 2 to 10 units of α-methylstyrene and from 8 to 51 units of styrene. The total number of matrix elements is 9 × 44 = 396, of which only 232 are occupied.

A graphical representation of these matrices, as three dimensional surfaces, can be seen in Figure 2A,B. In both parts, the shapes of the distribution functions are well defined in the high intensity (probability) regions and become blurred for lower intensities. One can also easily see the missing parts of the surfaces.

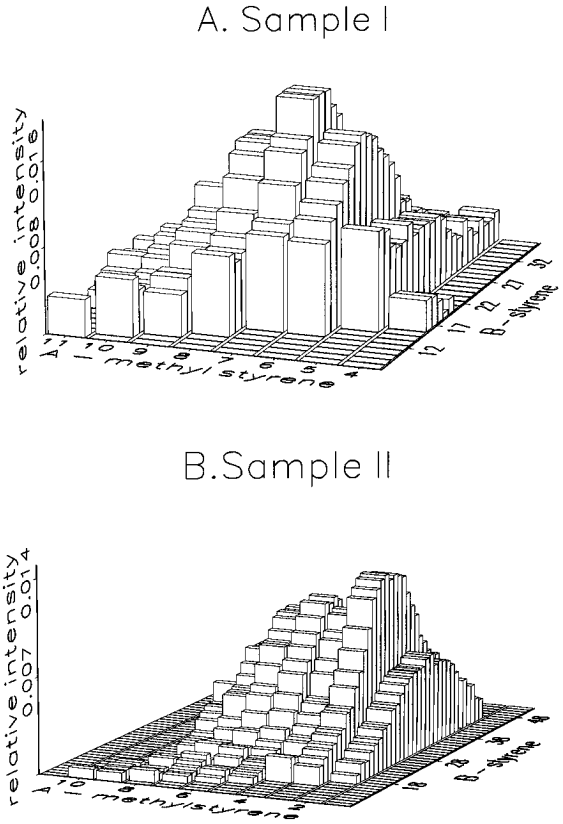

Figure 2. Experimental normalized distribution of units, $\Gamma_{exp}(n_{i_A}^A,n_{i_B}^B)$. (A) Sample I. (B) Sample II.

Experimental Marginal Probabilities. To verify the assumption of the random coupling hypothesis, which states that the molecular weights of individual parts are not correlated, the experimental marginal probabilities for the polymers studied were calculated. This was done by summing all the terms in columns to obtain the vector of the marginal probability[10] for part A:

$$\Gamma_{exp}^A(n_{i_A}^A) = \sum_{i_n=1}^{N_a} \Gamma_{exp}(n_{i_A}^A,n_{i_B}^B) \qquad (2)$$

The vector of marginal probability for part B was obtained by adding all the terms in rows:[10]

$$\Gamma_{exp}^B(n_{i_B}^B) = \sum_{i_A=1}^{N_A} \Gamma_{exp}(n_{i_A}^A,n_{i_B}^B) \qquad (2A)$$

If a block copolymer of the (poly A−poly B) type has a structure described by the random coupling statistics, i.e., the distribution of molecular weight of part A is independent of the distribution of molecular weight of part B, then the distribution function $\Gamma_{exp}(n_{i_A}^A,n_{i_B}^B)$ can be represented as a product of two marginal distributions:[10]

$$\Gamma_{exp}^{calc}(n_{i_A}^A,n_{i_B}^B) = \Gamma_{exp}^A(n_{i_A}^A)\Gamma_{exp}^B(n_{i_B}^B) \qquad (3)$$

Figure 3 demonstrates that this is really the case for sample I. This figure presents cuts through the three

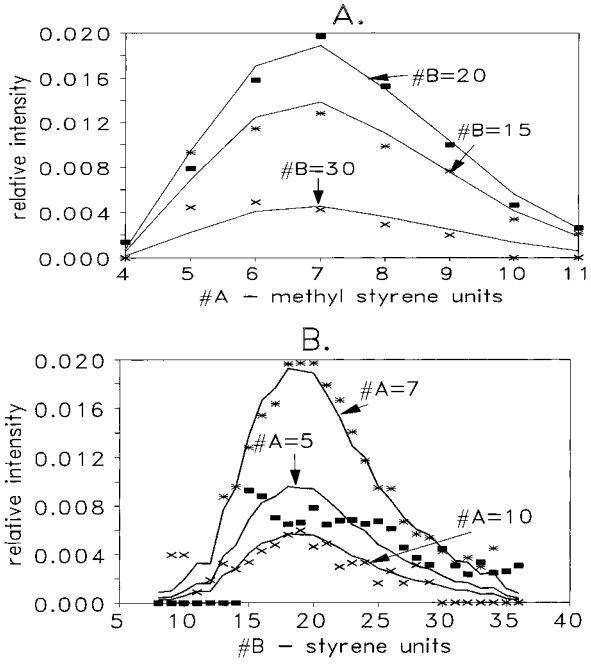

Figure 3. Comparison of the experimental $\Gamma_{exp}(n_{i_A}^A, n_{i_B}^B)$ and calculated $\Gamma_{exp}^A(n_{i_A}^A)\Gamma_{exp}^B(n_{i_B}^B)$ relative intensities for sample I. (A) Projections on the A-axis. (B) Projections on the B-axis. Markers, experimental data; lines, calculated values.

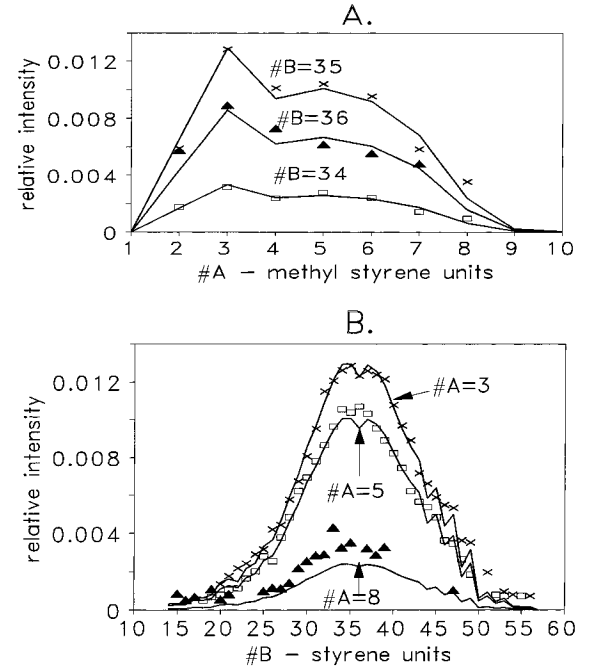

Figure 4. Comparison of the experimental $\Gamma_{exp}(n_{i_A}^A, n_{i_B}^B)$ and calculated $\Gamma_{exp}^A(n_{i_A}^A)\Gamma_{exp}^B(n_{i_B}^B)$ relative intensities for sample II. (A) Projections on the A-axis. (B) Projections on the B-axis. Markers, experimental data; lines, calculated values.

dimensional surface parallel to the A-axis (Figure 3A) or to the B-axis (Figure 3B). The calculated relative intensities reproduce well the shapes of the experimental values. Naturally, some smoothing in the lower intensity areas is observed. Despite this, it is obvious that the eq 3 holds. The values of $\Gamma_{exp}^B(n_{i_B}^B)$ were multiplied by 1.03 to account for the truncation of the border values of n_A in the experimental spectrum. Figure A in the supplementary material presents the three dimensional surface of $\Gamma_{exp}^{calc}(n_{i_A}^A, n_{i_B}^B)$ calculated from eq 3 for the same sample. There is very good

Table 7. Properties of the Studied Samples Calculated from the Experimental Distribution Functions $\Gamma_{exp}(n_{i_A}^A, n_{i_B}^B)$

	sample I		sample II	
	block A	block B	block A	block B
$\bar{n}_j$	7.3	20.4	4.6	35.8
$\bar{n}_j^w$	7.6	21.9	5.3	37.2
$\bar{n}_j^w/\bar{n}_j$	1.05	1.07	1.15	1.04
$\bar{x}_j = \frac{M_j^0 \bar{n}_j}{\bar{M}_n^{AB}}$	0.29	0.71	0.13	0.87
$\bar{M}_n^j$	859	2128	545	3728
$\bar{M}_w^j$	900	2280	628	3874
$\bar{M}_n^{AB}$	2987		4273	
$\bar{M}_w^{AB}$	3107		4411	
polydispersity factor	1.040		1.032	
$P/\bar{M}_w^{AB}$	−0.0073		−0.0016	
$Q/\bar{M}_w^{AB}$	0.0048		0.0023	

agreement between the experimental values (Figure 2A) and those calculated from eq 3 (Figure A). The estimated standard deviation of the relative intensity is 0.0013.

The same can be said about the second sample (see Figure 4 and Figure B in the supplementary material), even when the marginal distribution for the A part, $\Gamma_{exp}^A(n_{i_A}^A)$, is clearly bimodal, as shown in Figure 4A. The estimated standard deviation between the experimental and calculated values of the relative intensity is 0.0006.

The mass spectrometry technique gave us the unique opportunity to experimentally verify the random coupling hypothesis for this type of block copolymers. From now on, it can be treated as a physical phenomenon and not as an assumption.

The experimental distribution functions so obtained were used to calculate properties characterizing the chemical composition of both block copolymers. The following quantities were calculated and are presented in Table 7: (1) the average number of the segments j (j = A, B) in the block copolymer

$$\bar{n}_j = \frac{\sum_k^{N_A \times N_B} (n_k^j)\Gamma(n_k^A, n_k^B)}{\sum_k^{N_A \times N_B} \Gamma(n_k^A, n_k^B)} \tag{4}$$

(2) the weight average number of segments $\bar{n}_j^w$

$$\bar{n}_j^w = \frac{\sum_k^{N_A \times N_B} (n_k^j)^2\Gamma(n_k^A, n_k^B)}{\sum_k^{N_A \times N_B} \Gamma(n_k^A, n_k^B)} \tag{5}$$

(3) the polydispersity factor for a part j, $\bar{n}_j^w/\bar{n}_j$, (4) the chemical composition of part j

$$\bar{x}_j = \frac{M_j^0 \bar{n}_j}{\bar{M}_n^{AB}} \tag{6}$$

where $\bar{M}_n^{AB}$ is the number average molecular weight of the AB-block copolymer defined below (eq 8A), (5) the

number and the weight average molecular weight for part j

$$\bar{M}_n^j = \bar{n}_j M_j^0 \tag{7A}$$

$$\bar{M}_w^j = \bar{n}_j^w M_j^0 \tag{7B}$$

(6) the number and the weight average molecular weight of the block copolymer

$$\bar{M}_n^{AB} = \frac{\sum_k^{N_A \times N_B} (n_k^A M_A^0 + n_k^B M_B^0)\Gamma(n_k^A, n_k^B)}{\sum_k^{N_A \times N_B} \Gamma(n_k^A, n_k^B)} \tag{8A}$$

$$\bar{M}_w^{AB} = \frac{\sum_k^{N_A \times N_B} \Gamma(n_k^A, n_k^B)(n_k^A M_A^0 + n_k^B M_B^0)^2}{\sum_k^{N_A \times N_B} \Gamma(n_k^A, n_k^B)(n_k^A M_A^0 + n_k^B M_B^0)} \tag{8B}$$

(7) the polydispersity factor of the block copolymer, $\bar{M}_w^{AB}/\bar{M}_n^{AB}$, and (8) the heterogeneity parameters P and Q. The parameter P is a measure of mutual correlation of the distribution of molecular weights and chemical composition; the parameter Q characterizes the chemical heterogeneity of the copolymer.[1,11,12] These parameters are usually determined by light scattering.

$$P = \bar{x}_A \bar{x}_B [\bar{x}_A Y_A - \bar{x}_B Y_B] \bar{M}_n^{AB} \tag{9A}$$

$$Q = \bar{x}_A \bar{x}_B (\bar{M}_w^A + \bar{M}_w^B - \bar{M}_w^{AB}) \tag{9B}$$

where Ys are the molecular weight distribution indices, i.e., $Y_j = \bar{M}_w^j/\bar{M}_n^j - 1 = \bar{n}_j^w/\bar{n}_j - 1$.

It is interesting to analyze the properties of both samples. For sample I the average number of segments of type A (7.3) and B (20.4) agrees with the position of the maximum on the relative intensity surface. This means that, in principle, it would be possible to predict the shape of the composition distribution function from the values of $\bar{n}_j$ and $\bar{n}_j^w/\bar{n}_j$.

This is not the case for the second sample. Due to its bimodality, the average number of the A type segments (4.6) lies between two maxima for $n_A = 3$ and 5 on the relative intensity surface. It is not possible, therefore, to predict the distribution function from n_j and $\bar{n}_j^w/\bar{n}_j$. In general, properties listed in Table 7 give no indication that the composition distribution for sample II is bimodal. Only a graphical representation, as presented in Figure 2B, provides this additional information.

For both samples, the polydispersity factors for individual components are higher than for the whole copolymer. This proves experimentally the observation of Freyss et al.[13] that the molecular weight distribution of an AB-block polymer is always smaller than that of its most polydisperse precursor and often can be even smaller than either of the two precursors. Coupling of a shorter A-chain with a longer B-chain and *vice versa* narrows the molecular weight distribution but, as can be seen on Figure 2, it does not narrow the compositional heterogeneity.[14]

Analysis of Experimental Data: Poisson vs Schulz-Zimm (Γ) Model. It is commonly believed[15] that the distribution of units of anionic polymers is governed by the Poisson distribution:

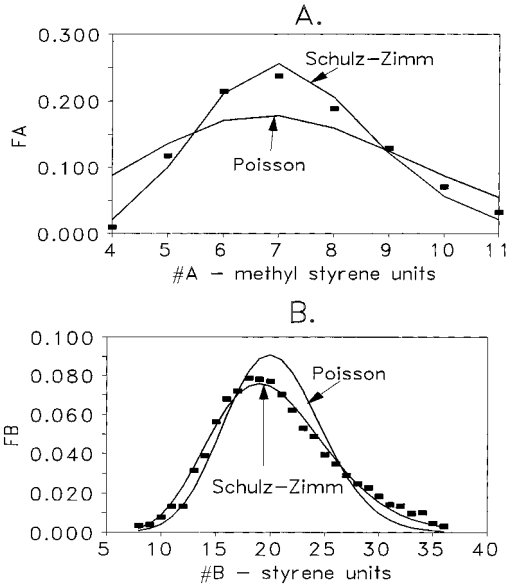

Figure 5. Sample I. Comparison of the experimental marginal distribution functions with the predictions of the Poisson and Schulz-Zimm models. (A) $\Gamma_{exp}^A(n_{i_A}^A)$. (B) $\Gamma_{exp}^B(n_{i_B}^B)$. Markers, experimental data; lines, calculated values.

$$\Gamma(n_k;\bar{n}) = \frac{(\bar{n} - 1)^{(n_k - 1)} \exp(1 - \bar{n})}{\Gamma^*(n_k)} \tag{10}$$

where n_k is the number of identical segments forming a particular block of the polymer and $\bar{n}$ is the average length of this block. $\Gamma^*(y)$ is the Γ function, which can be approximated either by a rather complex polynomial form or by Sterling's expansion.[16] As both approaches gave almost identical results for both cases considered in this paper, a numerically simpler Sterling's approximation was used:

$$\Gamma^*(y) = y^y \exp(-y)(2\pi/y)^{1/2} \tag{11}$$

The final form of eq 10 used to calculate the marginal probabilites was

$$\ln[\Gamma(n_k;\bar{n})] = (n_k - 1)\ln(\bar{n} - 1) + (1 - \bar{n}) + (0.5 - n_k)\ln(n_k) + n_k \tag{12}$$

The parameters needed for calculations ($\bar{n}_j$) were taken from Table 7. There was no fitting or fine tuning involved. The marginal probabilities, calculated from eq 12, were subsequently normalized to unity. The results for sample I are presented on Figure 5. The form of eq 10 indicates that the shape of the Poisson equation is determined solely by the average number of segments, $\bar{n}$. The width of the distribution is relatively broad for low values $\bar{n}$ and narrows significantly when $\bar{n}$ increases. The comparison of the experimental and calculated data of the marginal distribution for part A (which has a short average length of the chain with $\bar{n}_A$ equal to 7.3) shows that the distribution predicted by the Poisson equation is, in this case, too wide (Figure 5A). The agreement between the Poisson model and the experimental data is much better for the marginal distribution of the longer block B ($\bar{n}_B = 20.4$). However, the calculated distribution is, in this case, too narrow (Figure 5B). It became clear that another, more flexible, function was needed.

On the basis of the information available in the literature,[1,11] the Schulz-Zimm (Gamma) model was chosen.[17,18] Other distributions, like the Tung distribution[19] or the logarithmic−normal distribution, were also considered. However, it was shown[1,11] that all these distribution functions give virtually identical results for low polydispersity polymers. Both copolymers had low polydispersity factors (see Table 7). Therefore, a preference was given to the Schulz-Zimm (Gamma) distribution which has the form similar to the Poisson model with one additional parameter controlling the width of the distribution. As this equation is usually presented in a form suitable for the use of the molecular weight and the chemical composition as independent variables, it was modified to use instead the numbers of segments of parts A and B. The modified equation has the form

$$\Gamma(n_k;y,\bar{n}) = \frac{(y/\bar{n})^y}{\Gamma^*(y)} n_k^{y-1} \exp\left(-\frac{y n_k}{\bar{n}}\right) \qquad (13)$$

with the positive parameters y and $\bar{n}$ interrelated through

$$y = \frac{1}{(\bar{n}_w/\bar{n}) - 1} \qquad (14)$$

The Gamma function was again approximated by Sterling's expansion which gave the final form of eq 13 as

$$\ln[\Gamma(n_k;y,\bar{n})] = y + (y-1)\ln(n_k) - \frac{y n_k}{\bar{n}} - y\ln(\bar{n}) - 0.5\ln(2\pi) + 0.5\ln(y) \qquad (15)$$

The parameters needed for calculations (y_j and $\bar{n}_j$) were once more taken from Table 7.

It should be pointed out that this change of variables, from the molecular weight and chemical composition to the number of segments of parts A and B, gives a more general mathematical description and makes possible the comparison of composition distributions obtained for block polymers formed from units of different molecular weights.

Figure 5 shows very good agreement between the experimental values of the marginal distributions and those calculated from the Schulz-Zimm model. The three dimensional surface of the calculated number distribution function, depicted in Figure C in the supplementary material, proves the applicability of the model. The estimated standard deviation between values of the relative intensity calculated from the marginal probabilities and those obtained from the Schulz-Zimm model is 0.008.

The experimental marginal distribution $\Gamma^A_{exp}(n^A_{i_A})$ for sample II was clearly bimodal (see Figure 4A). Therefore, a linear combination of two Schulz-Zimm models had to be used:

$$\Gamma^A_{model}(n^A_{i_A}) = 1.05\left(\frac{\Gamma^A_{model}(3)}{\Gamma^A_{exp}(3)}\Gamma^A_1(n^A_{i_A}) + \frac{\Gamma^A_{model}(5)}{\Gamma^A_{exp}(5)}\Gamma^A_2(n^A_{i_A})\right) \qquad (16)$$

The parameters, y^i_A and $\bar{n}^i_A$ (where $i = 1$ or 2), that determine the shape of the Schulz-Zimm function were optimized to match the experimental marginal distribution function for part A. Table 8 lists them together with other characteristic parameters. The calculated marginal distributions $\Gamma^A_1(n^A_{i_A})$ and $\Gamma^A_2(n^A_{i_A})$ were normalized to adjust the calculated relative intensity to the experimental values for the two peaks at $n^A_{i_A} = 3$ and 5. The comparison of the calculated marginal distribution $\Gamma^A_{model}(n^A_{i_A})$ with the experimental marginal distribution $\Gamma^A_{exp}(n^A_{i_A})$ is presented on Figure 6A. There is an excellent agreement between both functions.

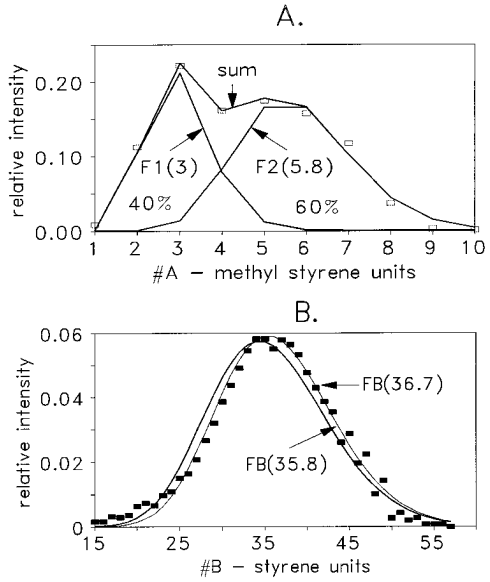

Figure 6. Sample II. Comparison of the experimental marginal distribution function with the prediction of the Schulz-Zimm model (A) $\Gamma^A_{exp}(n^A_{i_A})$ vs calculated superimposition of two Schulz-Zimm model (B) $\Gamma^B_{exp}(n^B_{i_B})$. Markers, experimental data; lines, calculated values.

Table 8. Characteristic Parameters of the Bimodal Distribution, $\Gamma^A_{exp}(n^A_A)$, for Sample II

parameter	$\Gamma^A_1(n^A_{i_A})$	$\Gamma^A_2(n^A_{i_A})$
$\bar{n}_j$	3.0	5.8
$\bar{n}^w_j$	3.2	6.1
$\bar{n}^w_j/\bar{n}_j$	1.07	1.06
$\bar{M}^j_n$	354.5	685.4
$\bar{M}^j_w$	377.6	723.1
y_j	15.4	18.2
$h_i = (y_j/\bar{n}_j)$	5.1	3.1

The area under the first curve $\Gamma^A_1(n^A_{i_A})$, with the maximum on $\bar{n}^1_A = 3$, comprises about 40% of the total area. The second curve $\Gamma^A_2(n^A_{i_A})$, with the maximum on $\bar{n}^2_A = 5.8$, contributes in 60% to the bimodal distribution function.

A likely explanation of the bimodality of the marginal distribution function for the precursor A (α-methylstyrene) in the ABA-block copolymer is the possibility of the termination of the polymerization reaction after the styrene addition but before the addition of the third block (the terminal segment of α-methylstyrene), i.e., the formation of the AB-diblock. For those polymer chains which did form the triblock, ABA, the average number of α-methylstyrene molecules that reacted was six. It is clear that the termination of the chain must have occurred in the third step of the polymerization process, i.e., after the styrene addition, otherwise no polystyrene would have been added to the α-methylstyrene. Our results indicate that **on average**, the first and the third blocks have the same length of about three units of α-methylstyrene. This validates, to a certain degree, the commonly used approximation of equal blocks,[11] which assumes that all precursor blocks of the A or B type have the same length in a given copolymer

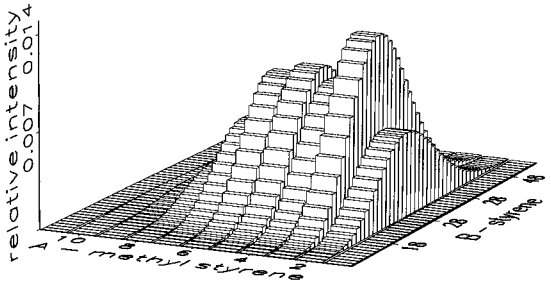

Figure 7. Three dimensional surface calculated from the Schulz-Zimm model, sample II.

molecule and different lengths in different molecules. In this approximation, the values of y_j should be independent of the number of blocks incorporated, while the values of the ratio $(y_j/\bar{n}_j)$ should be inversely proportional. Results presented in Table 8 seem to confirm the validity of this assumption. It is noteworthy that the commonly used approximation of equal blocks, which is usually applied to triblock copolymers prepared anionically by using such initiators as sodium naphthalene, is apparently valid also here for a monofunctional initiator system. This is probably related to the fact that the α-methylstyrene is above its ceiling temperature and the chains are, therefore, very short. The other possible reason is that the total α-methylstyrene monomer concentration does not change appreciably during the polymerization.

Figure 6B compares the experimental values of the marginal distribution function $\Gamma^{B}_{exp}(n^{B}_{i_B})$ with those calculated from the Schulz-Zimm model. As in all other cases, the parameters needed for calculations (y_j and $\bar{n}_j$) were taken from Table 7. There was no fitting or fine tuning involved. The agreement observed is good. There is some indication of bimodality of this function too, but the slight indent in the peak was produced by the experimental inaccuracy. The small peak of relative intensity of about 0.0033 for the (8,36) AB-pair was not resolved from its neighbor and therefore is absent from the AB matrix. This produced the indent of the same value on the marginal distribution function. It was impossible to reproduce this indent by any combination of two Schulz-Zimm distributions. Therefore, a unimodal function was assumed. A slight shift of the position of the maximum, $\bar{n}_B$, from 35.8 to 36.7 improves significantly the agreement between the calculated and the experimental values (Figure 6B). Nevertheless, the nonadjusted function was used for further calculations. The three dimensional surface of the number distribution function is depicted on Figure 7. Taking into account all the experimental noise, it resembles quite closely the experimental distribution function. The estimated standard deviation between the values of the relative intensity calculated from the experimental marginal distributions and those predicted by the Schulz-Zimm model is 0.005.

Breadth of Compositional Distributions. To visualize the breadth of the compositional distribution, the mole fractions of styrene, x_B for both samples studied was calculated. Figure 8A depicts the compositional distribution for sample I, determined from the experimental spectrum. Certain patterns emerge when scattered points are analyzed. The origin of these patterns is explained in Figure 8B, which presents the compositional distribution calculated from the Schulz-Zimm model. As can be seen, all the relative probabilities of the occurrence of the mole fraction of styrene, x_B,

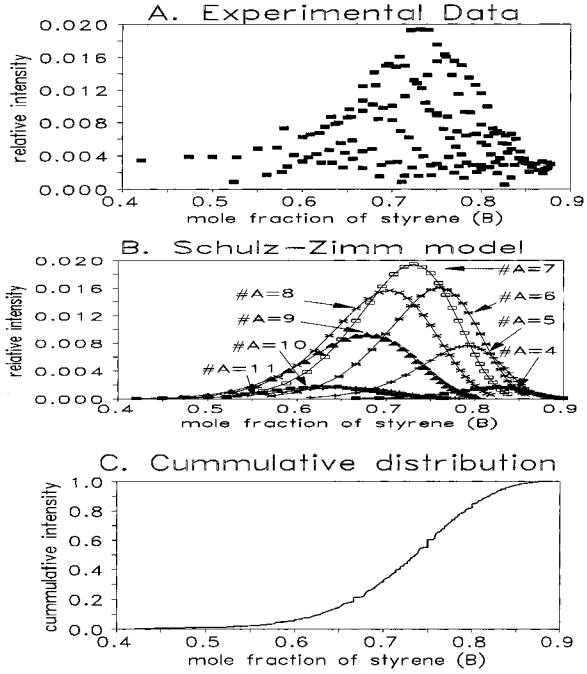

Figure 8. Sample I. (A) Experimental distribution of the chemical composition. (B) Compositional distribution calculated from the Schulz-Zimm model. (C) Experimental cumulative distribution function for the mole fraction of styrene, x_B.

corresponding to the same value of n_A, form a distribution resembling the Gaussian. Since many n_A values are possible, many of these distributions overlap.

In general, it is observed that despite a rather low value of the polydispersity factor of 1.04, the mole fraction of styrene varies from 0.42 to 0.88. The average value is 0.71. Figure 8C presents the cumulative distribution of the chemical composition. It is clear that it is difficult to treat this sample as compositionally homogeneous.

This trend is even more pronounced for the second sample. The calculated polydispersity factor is only 1.032, but the values of the mole fraction of styrene vary from 0.32 to almost 0.96 (see Figure 9). The average value is 0.87. As more than 99% of the sample has a mole fraction of styrene higher than 0.65, the compositional distribution presented in Figure 9 covers the range of x_B between 0.65 and 0.96. Once again, Figure 9A,B shows the overlap of multiple distributions. Only the mass spectrometry technique can provide this type of information.

Comparison with Size Exclusion Chromatography. One of the most frequently used techniques for the determination of the number-average and the weight-average molecular weight of a polymer is size exclusion chromatography (SEC). Therefore, the calculated averages obtained from the mass spectrometry data treatment (Table 7) were compared with the SEC results (Table 9).

The SEC results for the average molecular weights are lower by around 500 than those obtained from the MS technique. As this constitutes only about five styrene units, this difference is not large, since the SEC technique has limited accuracy for low molecular weight polymers.[20] In a previous study,[12] serious column adsorption problems were found for copolymers with short polystyrene blocks. Thus, we consider that the agreement between the two methods is satisfactory. Other results, similarly, show satisfactory agreement between SEC and MALDI/TOF spectrometry.

Table 9. Experimental Values of the Number-Average and Weight-Average Molecular Weight and of the Dispersity for the Analyzed Samples as Obtained by SEC Analysis

sample	z average molecular weight	number average molecular weight	weight average molecular weight	polydispersity
I	3240	2410	2760	1.14
II	5000	4190	4510	1.08

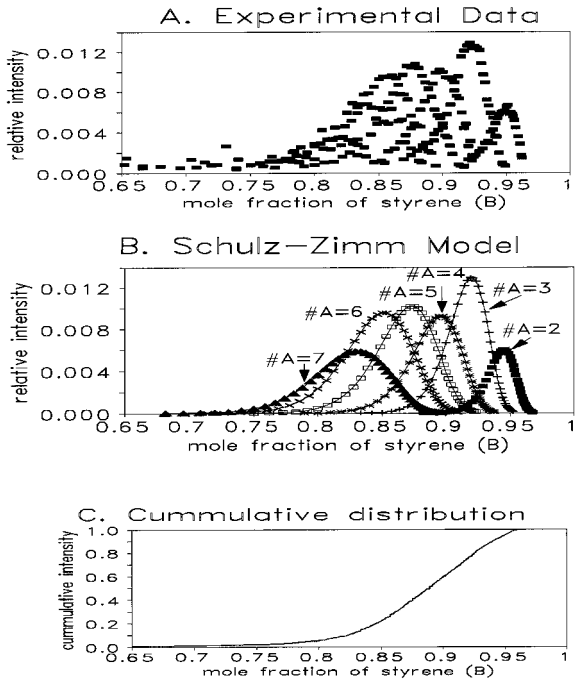

Figure 9. Sample II. (A) Experimental distribution of the chemical composition. (B) Compositional distribution calculated from the Schulz-Zimm model. (C) Experimental cumulative distribution function for the mole fraction of styrene, x_B.

Conclusions

Two samples of a block copolymer (α-methylstyrene−styrene), differing in molecular weight, were studied. It has been demonstrated that the mass spectroscopic technique, combined with ^{1}H-NMR spectroscopy, can be successfully used in the determination of the composition distribution of block copolymers. Using this method, it is possible to determine independently the molecular weight distribution of both parts forming a polymer.

A method for characterization of the MS peaks for copolymer is proposed. The correctness of the peak assignments was verified by comparing the obtained chemical compositions with values determined by ^{1}H-NMR spectroscopy.

The experimental composition distributions, determined by mass spectrometry, made possible the verification of the random coupling hypothesis, which obviously holds for the polymers studied. The assumption of equal blocks was also, in the statistical sense, validated.

In addition, it was observed that the polydispersity factors for individual blocks are higher than for the whole polymer, as has been suggested by Freyss et al.[13]

It was confirmed that block copolymers with narrow molecular weight distributions may, nevertheless, have broad and complex composition distributions.[1] The chemical composition can vary from 0.4 to 0.9, even though the polydispersity index for the whole polymer is only 1.04.

The commonly used Schultz-Zimm distribution model reproduced very well the experimental composition distributions.

The possibility of seeing directly the experimental composition distributions for block copolymers, formed from two precursors, opens the opportunity to study how different factors governing the polymerization process affect the final composition of a copolymer. The MS technique is a new and powerful tool in this study.

Acknowledgment. We are grateful to Dr. S. K. Wolk for the NMR spectrum of the second polymer sample and to Xing Fu Zhong for supplying us with polymer samples which were originally prepared for use in a different project.

Supporting Information Available: Figures of the calculated product of experimental marginal distributions of samples I and II and a three-dimensional surface calculated from the Schulz−Zimm model (3 pages). Ordering information is given on any current masthead page.

References and Notes

(1) Tanaka, T.; Omoto, M.; Donkai, N.; Inagaki, H. *J. Macromol. Sci.-Phys.* **1980**, *B17* (2), 211.
(2) Leng, M.; Benoit, H. *J. Polym. Sci.* **1962**, *57*, 263.
(3) Mori, S. *J. Appl. Polym. Sci.: Appl. Polym. Symp.* **1991**, *48*, 133.
(4) Trathnigg, B.; Yan, X. *J. Appl. Polym. Sci.: Appl. Polym. Symp.* **1993**, *52*, 193.
(5) Teramachi, S.; Hasegawa, A.; Shigekuni, Y.; Zenta, K.; Hashimoto, M. *J. Appl. Polym. Sci.: Appl. Polym. Symp.* **1990**, *45*, 87.
(6) Nguyen, D.; Zhong, X.-F.; Williams, C. E.; Eisenberg, A. *Macromolecules* **1994**, *27*, 5173.
(7) Nuwaysir, C. L.; Wilkins, C. L.; Simonsick, W. J. *J. Am. Soc. Mass Spectrom.* **1990**, *1*, 66−71.
(8) Viswanathan, K. V. *J. Appl. Polym. Sci.: Appl. Polym. Symp.* **1990**, *45*, 361.
(9) Danis, P. O.; Karr, D. E.; Simonsick, W. J., Jr.; Wu, D. T. *Macromolecules* **1995**, *28*, 1229.
(10) Kreysizg, E. *Advanced Engineering Mathematics*; John Wiley & Sons, Inc.: New York, 1993; Chapter 23.
(11) Stejskal, J.; Kratochvil, P. *Polym. J.* **1982**, 603.
(12) Zhong, X. F.; Varshney, S. K.; Eisenberg, A. *Macromolecules* **1992**, *25*, 7160.
(13) Freyss, D.; Rempp, P.; Benoit, H. *J. Polym. Sci. (Phys.)* **1969**, *B2*, 217.
(14) Kotaka, T.; Donkai, N.; Mix, T. I. *Bull. Inst. Chem. Res., Kyoto Univ.* **1974**, *52*, 332.
(15) Elias, H.-G. *Macromolecules. Structure and Properties*; Plenum Press: New York, 1977.
(16) *Handbook of mathematical functions with formulas, graphs, and mathematical tables*; Abramowitz, M., Steguin, I. A., Eds.; U.S. Govt. Print. Of.: Washington, DC, 1966.
(17) Schulz, G. V. *Z. Phys. Chem.* **1939**, *B43*, 25.
(18) Zimm, B. H. *J. Chem. Phys.* **1948**, *16*, 1093, 1099.
(19) Tung, L. H. *J. Polym. Sci.* **1956**, *20*, 495.
(20) Procházka, A.; Kratochvíl, P. *J. Appl. Polym. Sci.* **1987**, *34*, 2325.

MA9516394